Complexities of Microtubule Population Dynamics within the Mitotic Spindle

Aaron R. Tipton* and Gary J. Gorbsky

Cell Cycle and Cancer Biology Research Program, Oklahoma Medical Research Foundation, Oklahoma City, OK 73104, USA

*Address correspondence to: Aaron R. Tipton (aaron-tipton@omrf.org)

Running Head: Spindle microtubule population dynamics

Abbreviations used: PAGFP, photoactivatable green fluorescent protein; RNAi, RNA interference; STLC, S-trityl-L-cysteine;

Characters: 24,892

Abstract

The mitotic spindle functions to move chromosomes to alignment at metaphase, then segregate sister chromatids during anaphase. Analysis of spindle microtubule kinetics utilizing fluorescence dissipation after photoactivation described two main populations, a slow and a fast turnover population, historically taken to reflect kinetochore versus non-kinetochore microtubules respectively. This two component demarcation seems likely oversimplified. Microtubule turnover may vary among different spindle microtubules, regulated by spatial distribution and interactions with other microtubules and with organelles such as kinetochores, chromosome arms, and the cell cortex. How turnover among various spindle microtubules is differentially regulated and its significance remains unclear. We tested the concept of kinetochore versus non-kinetochore microtubules by disrupting kinetochores through depletion of the Ndc80 complex. In the absence of functional kinetochores, microtubule dynamics still exhibited slow and fast turnover populations, though proportions and timings of turnover were altered. Importantly, the data obtained following Hec1/Ndc80 depletion suggests other sub-populations, in addition to kinetochore microtubules, contribute to the slow turnover population. Further manipulation of spindle microtubules revealed a complex landscape. Dissection of the dynamics of microtubule populations will provide a greater understanding of mitotic spindle kinetics and insight into roles in facilitating chromosome attachment, movement, and segregation during mitosis.

Introduction

The mitotic spindle is a highly dynamic, spatially organized array of microtubules that functions to orchestrate equal distribution of genetic material to daughter cells. Microtubules comprising the mammalian mitotic spindle at metaphase are often broadly classified into three categories. Kinetochore fiber microtubules comprise a dense bundle extending from poles to kinetochores with many making direct contact with kinetochores at their plus ends. Kinetochore fiber microtubules play the major role in chromosome movement and regulating the spindle checkpoint through interactions with kinetochores. Astral microtubules emanate from spindle poles extending toward the cell cortex and are important for spindle positioning. Interpolar microtubules extend from the poles to interdigitate at the spindle equator. Early examination of spindle microtubule dynamics through fluorescence dissipation after photoactivation assays demonstrated that dissipation data were best fit by a double exponential curve [1]. Two populations of microtubules were detected, a fast turnover slow turnover population. These two populations were equated with non-kinetochore and kinetochore microtubules, which have been widely reported in early electron microscopic studies [2-8]. However, it seems likely that the true understanding of spindle microtubule dynamics would include more than two populations. For example, electron microscopy identifies within kinetochore fibers microtubules that reach from pole to kinetochore, others linked to either the pole or kinetochore with the other end free, and microtubules with two free ends [4, 9]. Potentially all may exhibit different dynamics within the fiber. To better evaluate the multiplicity of microtubule turnover within metaphase mitotic spindles, we carried out photoactivation experiments while manipulating populations of microtubules.

Results and Discussion

Mitotic spindles in cells lacking functional kinetochores still reveal fast and slow turnover microtubule populations

Kinetochore microtubules are one of three populations of microtubules suggested to comprise the mitotic spindle. Early fluorescence dissipation after photoactivation observations of spindle microtubule dynamics suggested the slow turnover population of microtubules within the spindle was comprised chiefly of kinetochore microtubules based on observations demonstrating they are more stable than non-kinetochore microtubules [1, 4, 8, 10-13]. The Ndc80 complex, comprised of Hec1/Ndc80, Nuf2, Spc24, and Spc25 is the primary microtubule binding component at kinetochores [14-17]. Therefore, if only two populations, kinetochore and non-kinetochore microtubules, exist within the central spindle of metaphase cells, disruption of the Ndc80 complex should eliminate the slow turnover population. To test this, we measured fluorescence dissipation after photoactivation of microtubules in U2OS cells stably expressing photoactivatable GFP (PAGFP)-tubulin and mCherry-Tubulin. Cells transfected with either control or Hec1 siRNA, to prevent kinetochore-microtubule interaction, were analyzed. 10 μM MG132 was included to prevent mitotic exit. Only cells entering mitosis during the time frame of imaging were photoactivated because we have found tubulin turnover is affected by prolonged metaphase arrest (data not shown). Mitotic spindles were located by mCherry-Tubulin fluorescence. A bar-shaped region within the spindle on one side of the metaphase plate was illuminated and time-lapse images were acquired as described in methods section. Representative images depict fluorescence in pre- and post-photoactivated cells and the mid-volume mCherry-Tubulin plane (Fig. 1, Top). Plots were generated for control and Hec1-depleted cells as described in methods section. As determined in previous photoactivation experiments with spindle microtubules [1] data from control cells were best fit by double exponential curves with the formula $F = A1 \times \exp(-k1 \times t) + A2 \times \exp(-k2 \times t)$ where A1 and A2 represent the percent total fluorescence contribution of the fast turnover and slow turnover microtubule populations, and k1 and k2 represent the respective decay rate constants (Fig. 1, bottom). However, even though Hec1 depletion would be expected to largely eliminate microtubule attachment at kinetochores, photoactivation data remained best fit by the double exponential suggesting that photoactivation still detected two major populations of microtubules (Fig. 1, bottom). Fitting to single and triple exponential curves resulted in poorer R^2 values ($R^2 < 0.990$). Successful Hec1 depletion was confirmed by comparing fluorescent DNA morphology to known Hec1 depletion phenotypes (Fig. S1) [15, 18]. While the total fluorescence contribution of the fast and slow turnover microtubule populations in control cells was measured to be 39% ± 2.7% and 61% ± 2.7%, respectively, cells depleted of Hec1 had both an increase in the fast turnover population to 52% ± 6.4% and a decrease in the slow turnover population to 48% ± 6.4%. In Hec1-depleted cells a portion of the slow turnover microtubule population is reduced, and the fast turnover population increased. This suggests that mitotic spindles in cells unable to form end-on microtubule attachments (lacking kinetochore microtubules) are still comprised of multiple populations, fast turnover and slow turnover. When microtubule half-lives were examined, minor changes were observed between control and Hec1-depleted cells in the fast turnover population (Control RNAi $t_{1/2}$ = 9.4 ± 0.5 s; Hec1 RNAi $t_{1/2}$ = 12.9 ± 3.1 s). In contrast, the half-life of the slow turnover population significantly decreased after Hec1 depletion ($t_{1/2}$ = 3 ± 0.2 m) when compared with controls ($t_{1/2}$ = 6.4 ± 0.3 m) (Fig. 1, bottom). Together, the data above indicates the presence of a slow turnover population of microtubules in the mitotic spindle in the absence of Hec1 and kinetochore microtubules. This suggests that without kinetochore-attached microtubules, two populations remain detectable by photoactivation indicating that slow turnover microtubules include one of more populations that are not kinetochore bound, contrary to the current dogma.

The slow turnover microtubule population is affected by the loss of spindle bipolarity

Interpolar microtubules of opposite polarity that interdigitate plus ends near the spindle midline are another category of microtubules proposed to comprise the mitotic spindle. Early classification of mitotic spindle structure suggested that most non-kinetochore microtubules were interpolar microtubules, concluding that interpolar microtubules constituted the bulk of the mitotic spindle [2,

3, 7]. Later, the fast turnover population of microtubules within the mitotic spindle was inferred to be comprised of interpolar microtubules [1]. To remove interdigitating, interpolar microtubules from the mitotic spindle, cells were treated with the Eg5 inhibitor S-trityl-L-cysteine (STLC) (10 μM) to block bipolar spindle formation, or DMSO, leaving microtubules extending with uniform polarity from the centrosomes some of which are free in the cytoplasm while others interact with kinetochores lacking bipolar tension and chromosome arms. Cells were analyzed as described in Fig. 1. Representative images depict fluorescence in pre- and post-photoactivated cells and the mid-volume fluorescence mCherry-Tubulin plane (Fig. 2, Top). A double exponential curve best fit the resulting data (Fig. 2, Bottom). While the total fluorescence contribution of the fast and slow turnover microtubule populations in control cells was measured to be 30% ± 3.7% and 70% ± 3.7%, respectively, cells treated with STLC had both an increase in the fast turnover microtubule population to 37% ± 6.6% and a decrease in the slow turnover microtubule population to 64% ± 6.5%. This suggests that in cells treated with STLC a portion of the slow turnover microtubule population is reduced, resulting in an increase in fast turnover population. Thus, in cells prevented from forming bipolar spindles (lacking interdigitating interpolar microtubules) microtubules are still comprised of fast and slow turnover populations. When microtubule half-lives were examined, minor changes were observed between control and STLC treated cells in the fast turnover population (Control $t_{1/2}$ = 7.3 ± 1.4 s; STLC $t_{1/2}$ = 5.3 ± 1.6 s). In contrast, the half-life of the slow turnover population significantly decreased following STLC treatment ($t_{1/2}$ = 3.5 ± 0.5 m) when compared with controls ($t_{1/2}$ = 6.4 ± 0.2 m) (Fig. 2, Bottom). Contrary to previous assumptions, the data are consistent with the interpretation that interdigitating interpolar microtubules also constitute a portion of the slow turnover population within the mitotic spindle in cells treated with STLC. However, we cannot rule out that the decrease in the $t_{1/2}$ of the slow turnover population or the increase in the fast turnover population may in part be due to microtubules attached to kinetochores lacking bipolar attachment and tension, resulting in decreased stability. Similarly, increases in the proportion of astral microtubules may account for the increase in the fast turnover population. Unfortunately our efforts to reduce both kinetochore microtubules and interdigitating interpolar microtubules were unsuccessful. Hec1-depleted cells treated with 100 μM Monastrol formed bipolar spindles. Representative images depict fluorescence in pre- and post-photoactivated cells and the mid-volume fluorescence mCherry-Tubulin and DNA plane (Fig. S2). This finding shows that functional kinetochores are required to collapse spindles in mitotic cells treated with Eg5 inhibitors. This result is consistent with previous studies [19, 20].

Both fast and slow turnover microtubule populations are sensitive to decreased temperature

A well-established characteristic of spindle microtubules in cell culture models is the sensitivity of stability to changes in temperature [1, 3, 4, 21]. In the LLC-PK cell line, decreases in temperature resulted in increases in the $t_{1/2}$ of the slow turnover microtubule population, with no major effect on the $t_{1/2}$ of the fast turnover population [1]. This study also reported an overall increase in the fluorescence contribution of the fast turnover population and decrease of the slow turnover population following reductions in temperature. We sought to examine the effects of reductions in temperature on spindle microtubule dynamics in the U2OS cell line. Cells were imaged at 37°C (Control) as described above or at room temperature (22°C-25°C) (Low Temperature) as described in methods section. Representative images depict fluorescence in pre- and post-photoactivated cells and the mid-volume fluorescence mCherry-Tubulin plane (Fig. 3, Top). A double exponential curve best fit the resulting data (Fig. 3, Bottom). In contrast to the report from Zhai et al., we detected only minor differences in the fluorescence contribution of fast and slow turnover microtubule populations when comparing control cells to cells imaged at low temperature. The fast and slow turnover populations for control cells were 35% ± 1.9% and 65% ± 1.9%, respectively, while the fast and slow turnover populations for cells imaged at low temperature were 38% ± 2.6% and 61% ± 2.7%, respectively. When microtubule half-lives were

examined, major increases were observed between control cells and cells imaged at low temperature in both the fast turnover population (Control $t_{1/2}$ = 7 ± 1.9 s; Low Temperature $t_{1/2}$ = 15.7 ± 2.6 s) and the slow turnover population (Control $t_{1/2}$ = 4.6 ± 1.9 m; Low Temperature $t_{1/2}$ = 14.4 ± 2.7 m) (Fig. 3, Bottom). This is in contrast to the observations made by Zhai et al., which only saw increases in the $t_{1/2}$ of the slow turnover microtubule population. One potential explanation for the discrepancies could be due to differences in cell type. Additionally, advances in imaging technology may have permitted us to achieve higher temporal resolution allowing detection of differences in half-life of the fast turnover microtubule population.

The slow turnover microtubule population is sensitive to Aurora B kinase inhibition

Aurora B kinase is an important regulator of kinetochore-microtubule attachment [22-26]. Aurora B responds to improper microtubule attachment to kinetochores by phosphorylating the N-terminal tail of Hec1/Ndc80, which reduces microtubule binding affinity. A previous report demonstrated in the PtK1 cell line that inhibition of Aurora B kinase activity via the small molecule ZM447439 caused an extensive increase (over seven-fold) in the $t_{1/2}$ of the slow turnover microtubule population, with no major effect on the $t_{1/2}$ of the fast turnover population when compared to control metaphase cells [24]. We in turn sought to examine the effects of Aurora B kinase inhibition on spindle microtubule dynamics in the U2OS cell line. To inhibit Aurora B kinase activity cells were treated with either 3 μM ZM447439 or DMSO along with 10 μM MG132 to prevent mitotic exit. Cells were then analyzed as described above. Representative images depict fluorescence in pre- and post-photoactivated cells and the mid-volume fluorescence mCherry-Tubulin plane (Fig. 4, Top). A double exponential curve best fit the resulting data (Fig. 4, Bottom). While the total fluorescence contribution of fast and slow turnover populations in control cells was measured as 42% ± 1.2% and 58% ± 1.2%, respectively, cells treated with ZM447439 had a decrease in the fast turnover population to 37% ± 3.2% and increase in the slow turnover population to 63% ± 3.2%. This change is consistent with the role of Aurora B kinase in destabilizing kinetochore-microtubule attachments. When microtubule half-lives were examined, minor changes were observed between control and ZM447439 treated cells in the fast turnover population (Control $t_{1/2}$ = 9.8 ± 0.9 s; ZM447439 $t_{1/2}$ = 11.1 ± 0.5 s). In contrast, the half-life of the slow turnover population significantly increased following ZM447439 treatment ($t_{1/2}$ = 10.5 ± 0.8 m) when compared with controls ($t_{1/2}$ = 6.1 ± 0.7 m) (Fig. 4, Bottom). In partial agreement with Cimini et al., our microtubule half-life observations indicate the stability of kinetochore-microtubule attachments (a portion of the slow turnover microtubule population) increase following inhibition of Aurora B kinase activity. However, slow turnover microtubules displayed a much higher degree of stability following Aurora B kinase inhibition in PtK1 cells when compared to U2OS cells.

Aurora B kinase regulates the stability of non-kinetochore, slow turnover microtubules

To further examine the role Aurora B kinase activity plays in regulating spindle microtubule dynamics during mitosis, Aurora B kinase activity was inhibited in cells depleted of Hec1/Ndc80. We hypothesized that if Aurora B solely regulated kinetochore microtubules, then Aurora B inhibition should not alter spindle microtubule dynamics in cells depleted of functional kinetochores. To test this, cells were transfected with control siRNA followed by DMSO treatment or Hec1 siRNA followed by 3 μM ZM447439 treatment and analyzed as described above. 10 μM MG132 was included to prevent mitotic exit. Representative images depict fluorescence in pre- and post-photoactivated cells and the mid-volume fluorescence mCherry-Tubulin plane (Fig. 5, Top). A double exponential curve best fit the resulting data (Fig. 5, Bottom). We did not detect significant differences in the fluorescence contribution of fast and slow turnover populations when comparing control cells to cells depleted of Hec1 followed by ZM447439 treatment. The fast and slow turnover populations for control cells were 41% ± 2% and 59% ± 2.2%, respectively. While the fast and slow turnover populations for cells depleted of Hec1 followed by ZM447439 treatment were 42% ± 3.5% and 58% ± 3.5%, respectively. When microtubule half-lives were examined,

minor changes were observed between control cells and cells depleted of Hec1 followed by ZM447439 treatment in the fast turnover population (Control RNAi $t_{1/2}$ = 8.5 ± 0.1 s; Hec1 RNAi + ZM447439 $t_{1/2}$ = 9.1 ± 2 s). Strikingly however, the half-life of the slow turnover population significantly decreased in cells depleted of Hec1 followed by ZM447439 treatment ($t_{1/2}$ = 1.6 ± 0.1 m) when compared with controls ($t_{1/2}$ = 7.2 ± 0.6 m) (Fig. 5, Bottom). The half-life of the slow turnover population in cells depleted of Hec1 followed by ZM447439 treatment was also significantly decreased when compared to cells depleted of Hec1 alone (Hec1 RNAi $t_{1/2}$ = 3 ± 0.2 m; Hec1 RNAi + ZM447439 $t_{1/2}$ = 1.6 ± 0.1 m). Together these data suggest that Aurora B kinase plays roles in destabilizing slow turnover microtubules at kinetochores and other slow turnover microtubules within the mitotic spindle (comparing ZM447439 treatment alone and Hec1 depletion followed by ZM447439 treatment to their respective controls). One potential mechanism by which Aurora B kinase plays a role in stabilizing slow turnover microtubules is via regulation of localization and activity of microtubule depolymerases, such as the kinesin 13 family [19, 27-33]. However, we cannot rule out other potential mechanisms by which Aurora B kinase functions in stabilizing slow turnover microtubule populations.

The mitotic spindle is essential in the equal distribution of genetic material during mitosis. Early studies examining spindle microtubule dynamics determined the existence of two populations within the mitotic spindle [1]. A fast population that turns over in seconds and a slow population that turns over in minutes. These two populations were termed non-kinetochore microtubules (comprised of interdigitating interpolar microtubules) and kinetochore microtubules (comprised of microtubules attached to kinetochores), respectively. However, this nomenclature arose from observations indicating that microtubules attached to kinetochores displayed increased levels of stability while non-kinetochore microtubules represent the bulk of microtubules that constitute the mitotic spindle [1-4, 7, 8, 10-13, 21]. In this study, we sought to determine if this assumption reflected an oversimplification and if mitotic spindle dynamics could be tracked through various manipulations to reveal multiple subpopulations. We targeted kinetochore fibers by depleting Hec1/Ndc80. In the absence of this major microtubule binding component at kinetochores, the slow turnover population was primarily affected resulting in both a decrease in fluorescence contribution and the $t_{1/2}$ (Fig. 1). Data obtained following Hec1/Ndc80 depletion was best fit by a double exponential curve, indicating the existence of multiple populations in the absence of kinetochore microtubules. This suggests that kinetochore fibers are not the sole population comprising slow turnover microtubules. To target interdigitating interpolar microtubules, Eg5 inhibition was used to prevent bipolar spindle formation and formation of interdigitating interpolar microtubules. In contrast to previous assumptions suggesting that interpolar microtubules comprise the non-kinetochore (or fast turnover) population, we found that STLC treatment decreased both the fluorescence contribution and $t_{1/2}$ of the slow turnover population (Fig. 2). However, we cannot rule out that the decrease in the $t_{1/2}$ of the slow turnover population or the increase in the fast turnover population may in part be due to microtubules interacting with kinetochores lacking bipolar attachment/tension, or with microtubules associating with chromosome arms. It is likely increases in the proportion of free astral microtubules may account for the increase in the fast turnover population. When spindle microtubule dynamics were examined in conditions of reduced temperature, we found increases in the $t_{1/2}$ of both the fast and slow turnover populations, with little change in the relative fluorescence contribution (Fig. 3). This was in contrast to previous observations reporting changes in the $t_{1/2}$ in the slow turnover population while the fluorescence contribution of the fast population increased [1]. However, these discrepancies may have been a result of differences in cell lines or advances in imaging technology. The well-recognized regulator of kinetochore-microtubule attachment, Aurora B kinase, was also analyzed for its role in regulating microtubule dynamics within the mitotic spindle. In partial agreement with a previous report [24], we found an increase in the $t_{1/2}$ of the slow turnover population following Aurora B kinase inhibition. However, the slow turnover population

in PtK1 cells displayed elevated levels of stability following Aurora B kinase inhibition compared to U2OS cells. This is consistent with the established role of Aurora B kinase in destabilizing incorrect microtubule-kinetochore attachments via phosphorylation of Hec1 [22-26]. In the absence of both Hec1 and Aurora B kinase activity, the $t_{1/2}$ of the slow turnover population was drastically decreased. This suggests Aurora B kinase not only functions in destabilizing incorrect microtubule attachments to kinetochores, but also plays a role in enhancing microtubule stability of other populations within the mitotic spindle. A role for Aurora B kinase in regulating the localization and activity of microtubule depolymerases, such as the kinesin 13 family, has been previously established [19, 27-33], and may constitute the underlying mechanism behind our observations. Yet, we cannot rule out alternative pathways by which Aurora B kinase activity promotes spindle microtubule stability. Together, this study demonstrated that the mitotic spindle is more complex than a fast turnover population comprised of non-kinetochore microtubules and a slow turnover population comprised of kinetochore microtubules. The mitotic spindle is likely comprised of multiple subpopulations. The identity of the fast turnover microtubule population within the mitotic spindle and mechanisms to manipulate its turnover (apart from reductions in temperature) remain elusive. Furthermore, tubulin itself can be post-translationally modified [34-40]. Examining how various post-translational modifications play a role in regulating spindle microtubule dynamics during mitosis will be of future interest. Additionally, fluorescence dissipation after photoactivation experiments in cell lines utilizing different combinations of tubulin isoforms will greatly expand our knowledge of spindle microtubule dynamics.

Materials and Methods

siRNA

The siRNA sequence (5'-GAGUAGAACUAGAAUGUGA-3') targeting Hec1 was synthesized by Qiagen. Non-targeting control siRNA was synthesized by Bioneer.

Cell culture, transfection, and drug treatments

U2OS cells stably expressing photoactivatable GFP-Tubulin (PAGFP-Tubulin) and mCherry-Tubulin (see acknowledgments) were cultured in DMEM with 10% fetal bovine serum (FBS) supplemented with penicillin and streptomycin, 20mM HEPES, and 0.1 mM nonessential amino acids (NEAA) at 37°C with 5% CO_2. For siRNA transfection, cells were transfected with 20 nM siRNA for 48 h using Lipofectamine RNAiMAX (Invitrogen) according to the manufacturer's protocol. To inhibit Aurora B activity, cells were treated with 3 μM ZM447439. 10 μM MG132 was also added to prevent mitotic exit. S-trityl-L-cysteine (STLC) or Monastrol was used at 10 μM and 100 μM respectively to induce monopolar spindles. Taxol was used at 10 μM. All drugs were added 30 min prior to imaging. SiR-DNA (Cytoskeleton) was used at 500 nM to label DNA according to the manufacturer's protocol.

Photoactivation

PAGFP-Tubulin and mCherry-Tubulin expressing U2OS cells were grown on coverslips. To maintain appropriate pH levels and avoid evaporation during imaging, culture media was exchanged to Leibovitz's L-15 medium supplemented with 10% FBS, penicillin, and streptomycin, and the medium was overlaid with mineral oil. Cells were treated as detailed in the figure legends and imaged using a 100x, NA 1.4 objective on a Zeiss Axio Observer inverted microscope equipped with an objective heater, air curtain, Yokogawa CSU-22 (Yokogawa) spinning disk, Mosaic (digital mirror device, Photonic Instruments/Andor), a Hamamatsu ORCA-Flash4.0LT

(Hamamatsu Photonics), and Slidebook software (Intelligent Imaging Innovations). Photoactivation was achieved by targeting a selected area with filtered light from the HBO 100 via the Mosaic, and confocal GFP images (19 Z planes across 8 μm (0.5 μm/plane)) were acquired at 15 sec intervals for ~5 min. mCherry and SiR-DNA images were acquired at the mid volume Z plane. Only cells entering mitosis during imaging were photoactivated to ensure Tubulin turnover was not affected by prolonged mitotic arrest. To quantify fluorescence dissipation after photoactivation, we measured pixel intensities within an area surrounding the region of highest fluorescence intensity and background subtracted using an area from the nonactivated half spindle using MetaMorph software. The values were corrected for photobleaching by determining the percentage of fluorescence loss during image acquisition after photoactivation in the presence of 10 μM Taxol. Fluorescence values were normalized to the first time-point after photoactivation for each cell and the average intensity at each time point was fit to a double exponential curve F = A1 x exp(-k1 x t) + A2 x exp(-k2 x t), using SigmaPlot (SYSTAT Software), where A1 and A2 represent the fast turnover and slow turnover microtubule populations with decay rates of k1 and k2, respectively. t is the time after photoactivation. The turnover half-life for each population of microtubules was calculated as ln2/k. XY scatter plots were generated using GraphPad Prism.

Acknowledgments

We would like to thank, Marvin Tanenbaum, Rene Medema, and Helder Maiato for providing the cell line used and John R. Daum for technical assistance. This work was supported by grant 5R35GM126980 from the National Institute of General Medical Sciences.

Literature Cited

1. Zhai, Y., Kronebusch, P.J., and Borisy, G.G. (1995). Kinetochore Microtubule Dynamics and the Metaphase-Anaphase Transition. Journal of Cell Biology *131*, 721-734.
2. McIntosh, J.R., Cande, W.Z., and Snyder, J.A. (1975). Structure and physiology of the mammalian mitotic spindle. Soc Gen Physiol Ser *30*, 31-76.
3. Rieder, C.L. (1981). Effect of Hypothermia (20-25-Degrees-C) on Mitosis in Ptk1 Cells. Cell Biol Int Rep *5*, 563-573.
4. Rieder, C.L. (1981). The structure of the cold-stable kinetochore fiber in metaphase PtK1 cells. Chromosoma *84*, 145-158.
5. Wise, D., Cassimeris, L., Rieder, C.L., Wadsworth, P., and Salmon, E.D. (1991). Chromosome Fiber Dynamics and Congression Oscillations in Metaphase Ptk2 Cells at 23-Degrees-C. Cell Motil Cytoskel *18*, 131-142.
6. Rieder, C.L. (1982). The Formation, Structure, and Composition of the Mammalian Kinetochore and Kinetochore Fiber. International Review of Cytology-a Survey of Cell Biology *79*, 1-58.
7. Mastronarde, D.N., Mcdonald, K.L., Ding, R., and Mcintosh, J.R. (1993). Interpolar Spindle Microtubules in Ptk Cells. Journal of Cell Biology *123*, 1475-1489.
8. Salmon, E.D., Goode, D., Maugel, T.K., and Bonar, D.B. (1976). Pressure-Induced Depolymerization of Spindle Microtubules .3. Differential Stability in Hela-Cells. Journal of Cell Biology *69*, 443-454.
9. McDonald, K.L., O'Toole, E.T., Mastronarde, D.N., and McIntosh, J.R. (1992). Kinetochore microtubules in PTK cells. J Cell Biol *118*, 369-383.
10. Salmon, E.D., McKeel, M., and Hays, T. (1984). Rapid rate of tubulin dissociation from microtubules in the mitotic spindle in vivo measured by blocking polymerization with colchicine. J Cell Biol *99*, 1066-1075.

11. Mitchison, T.J. (1988). Microtubule Dynamics and Kinetochore Function in Mitosis. Annu Rev Cell Biol *4*, 527-549.
12. Gorbsky, G.J., and Borisy, G.G. (1989). Microtubules of the Kinetochore Fiber Turn over in Metaphase but Not in Anaphase. Journal of Cell Biology *109*, 653-662.
13. Cassimeris, L., Rieder, C.L., Rupp, G., and Salmon, E.D. (1990). Stability of Microtubule Attachment to Metaphase Kinetochores in Ptk1 Cells. J Cell Sci *96*, 9-15.
14. Wei, R.R., Al-Bassam, J., and Harrison, S.C. (2007). The Ndc80/HEC1 complex is a contact point for kinetochore-microtubule attachment. Nat Struct Mol Biol *14*, 54-59.
15. DeLuca, J.G., Dong, Y.M., Hergert, P., Strauss, J., Hickey, J.M., Salmon, E.D., and McEwen, B.F. (2005). Hec1 and Nuf2 are core components of the kinetochore outer plate essential for organizing microtubule attachment sites. Mol Biol Cell *16*, 519-531.
16. McCleland, M.L., Kallio, M.J., Barrett-Wilt, G.A., Kestner, C.A., Shabanowitz, J., Hunt, D.F., Gorbsky, G.J., and Stukenberg, P.T. (2004). The vertebrate Ndc80 complex contains Spc24 and Spc25 homologs, which are required to establish and maintain kinetochore-microtubule attachment. Current Biology *14*, 131-137.
17. DeLuca, J.G., Gall, W.E., Ciferri, C., Cimini, D., Musacchio, A., and Salmon, E.D. (2006). Kinetochore microtubule dynamics and attachment stability are regulated by Hec1. Cell *127*, 969-982.
18. Martin-Lluesma, S., Stucke, V.M., and Nigg, E.A. (2002). Role of Hec1 in spindle checkpoint signaling and kinetochore recruitment of Mad1/Mad2. Science *297*, 2267-2270.
19. Knowlton, A.L., Vorozhko, V.V., Lan, W., Gorbsky, G.J., and Stukenberg, P.T. (2009). ICIS and Aurora B coregulate the microtubule depolymerase Kif2a. Curr Biol *19*, 758-763.
20. Ganem, N.J., and Compton, D.A. (2004). The KinI kinesin Kif2a is required for bipolar spindle assembly through a functional relationship with MCAK. Journal of Cell Biology *166*, 473-478.
21. Brinkley, B.R., and Cartwright, J., Jr. (1975). Cold-labile and cold-stable microtubules in the mitotic spindle of mammalian cells. Ann N Y Acad Sci *253*, 428-439.
22. Murata-Hori, M., and Wang, Y.L. (2002). The kinase activity of aurora B is required for kinetochore-microtubule interactions during mitosis. Current Biology *12*, 894-899.
23. Cheeseman, L.M., Anderson, S., Jwa, M., Green, E.M., Kang, J.S., Yates, J.R., Chan, C.S.M., Drubin, D.G., and Barnes, G. (2002). Phospho-regulation of kinetochore-microtubule attachments by the aurora kinase Ipl1p. Cell *111*, 163-172.
24. Cimini, D., Wan, X., Hirel, C.B., and Salmon, E.D. (2006). Aurora kinase promotes turnover of kinetochore microtubules to reduce chromosome segregation errors. Curr Biol *16*, 1711-1718.
25. Pinsky, B.A., Kung, C., Shokat, K.M., and Biggins, S. (2006). The Ipl1-Aurora protein kinase activates the spindle checkpoint by creating unattached kinetochores. Nat Cell Biol *8*, 78-83.
26. Welburn, J.P.I., Vleugel, M., Liu, D., Yates, J.R., Lampson, M.A., Fukagawa, T., and Cheeseman, I.M. (2010). Aurora B Phosphorylates Spatially Distinct Targets to Differentially Regulate the Kinetochore-Microtubule Interface. Mol Cell *38*, 383-392.
27. Andrews, P.D., Ovechkina, Y., Morrice, N., Wagenbach, M., Duncan, K., Wordeman, L., and Swedlow, J.R. (2004). Aurora B regulates MCAK at the mitotic centromere. Dev Cell *6*, 253-268.
28. Lan, W.J., Zhang, X., Kline-Smith, S.L., Rosasco, S.E., Barrett-Wilt, G.A., Shabanowitz, J., Walczak, C.E., and Stukenberg, P.T. (2004). Aurora B phosphorylates centromeric MCAK and regulates its localization and microtubule depolymerization activity. Current Biology *14*, 273-286.
29. Ohi, R., Sapra, T., Howard, J., and Mitchison, T.J. (2004). Differentiation of cytoplasmic and meiotic spindle assembly MCAK functions by aurora B-dependent phosphorylation (Vol 15, pg 2895, 2004). Mol Biol Cell *15*.
30. Knowlton, A.L., Lan, W.J., and Stukenberg, P.T. (2006). Aurora B is enriched at merotelic attachment sites, where it regulates MCAK. Current Biology *16*, 1705-1710.

31. Sampath, S.C., Ohi, R., Leismann, O., Salic, A., Pozniakovski, A., and Funabiki, H. (2004). The chromosomal passenger complex is required for chromatin-induced microtubule stabilization and spindle assembly. Cell *118*, 187-202.
32. Ohi, R., Coughlin, M.L., Lane, W.S., and Mitchison, T.J. (2003). An inner centromere protein that stimulates the microtubule depolymerizing activity of a Kinl kinesin. Dev Cell *5*, 309-321.
33. Bakhoum, S.F., Thompson, S.L., Manning, A.L., and Compton, D.A. (2009). Genome stability is ensured by temporal control of kinetochore-microtubule dynamics. Nat Cell Biol *11*, 27-U51.
34. Magiera, M.M., and Janke, C. (2014). Post-translational modifications of tubulin. Curr Biol *24*, R351-354.
35. Song, Y., and Brady, S.T. (2015). Post-translational modifications of tubulin: pathways to functional diversity of microtubules. Trends Cell Biol *25*, 125-136.
36. Yu, I., Garnham, C.P., and Roll-Mecak, A. (2015). Writing and Reading the Tubulin Code. J Biol Chem *290*, 17163-17172.
37. Strzyz, P. (2016). Post-translational modifications: Extension of the tubulin code. Nat Rev Mol Cell Biol *17*, 609.
38. Wloga, D., Joachimiak, E., and Fabczak, H. (2017). Tubulin Post-Translational Modifications and Microtubule Dynamics. Int J Mol Sci *18*.
39. Barisic, M., Sousa, R.S.E., Tripathy, S.K., Magiera, M.M., Zaytsev, A.V., Pereira, A.L., Janke, C., Grishchuk, E.L., and Maiato, H. (2015). Microtubule detyrosination guides chromosomes during mitosis. Science *348*, 799-803.
40. Barisic, M., and Maiato, H. (2016). The Tubulin Code: A Navigation System for Chromosomes during Mitosis. Trends in Cell Biology *26*, 766-775.

Figure 1

Control RNAi + MG132

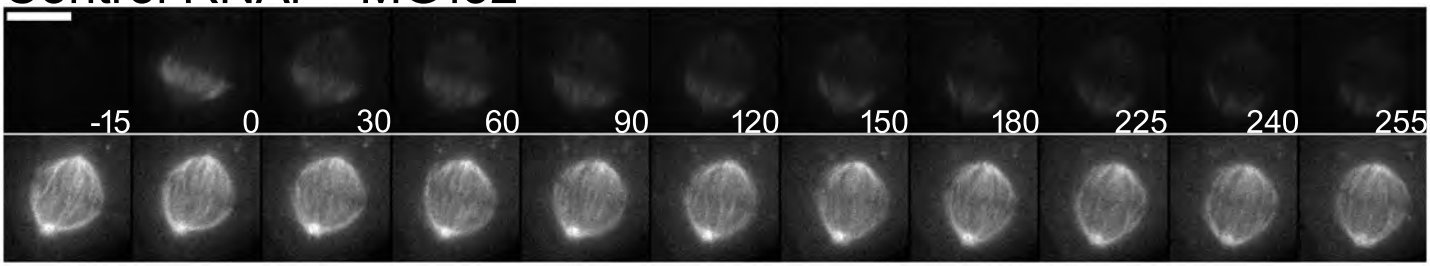

Hec1 RNAi + MG132

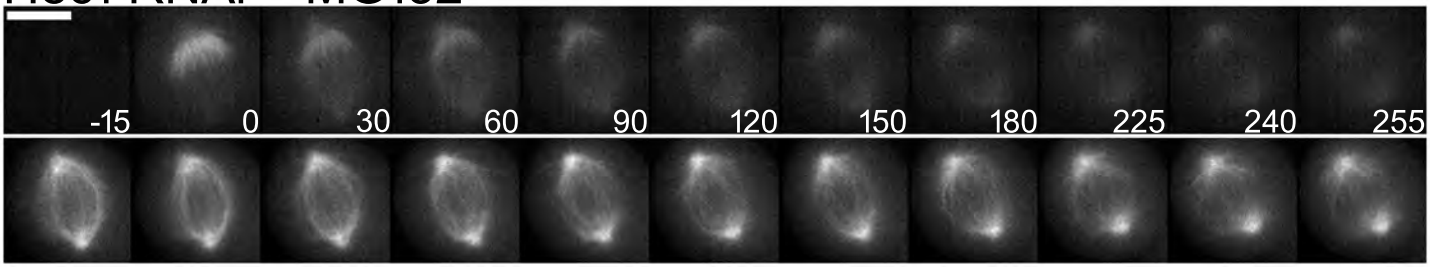

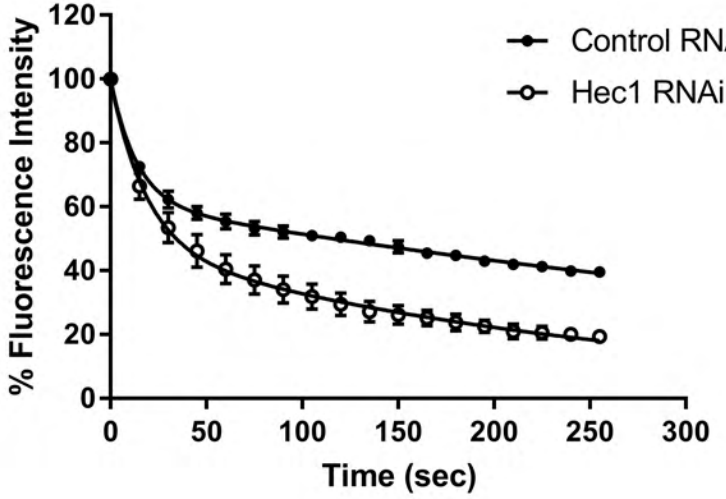

	Fast MT Population		Slow MT Population			
RNAi	%	$T_{1/2}$ (sec)	%	$T_{1/2}$ (min)	R^2	N
Control	39	9.4	61	6.4	0.999	19
Hec1	52	12.9	48	3	0.998	20

Figure 1. End-on attached microtubules comprise only a portion of the slow turnover microtubule population. (Top) Select frames from live cell imaging of Tubulin photoactivation in U2OS cells stably expressing photoactivatable GFP-Tubulin and mCherry-Tubulin following transfection with either control or Hec1 siRNA along with 10 μm MG132 treatment to prevent mitotic exit. mCherry-Tubulin frames are from the mid-volume plane. Control cells were imaged at metaphase. Time, sec. Bar, 10 μm. (Bottom) Fluorescence dissipation after photoactivation. The filled and unfilled circles represent the average values recorded at each time point after photoactivation. Bars represent SEM. Control n = 19 cells, Hec1 n = 20 cells from three independent experiments. Lines indicate fitted curves (Control RNAi R^2 = 0.999; Hec1 RNAi R^2 = 0.998).

Figure 2

Control

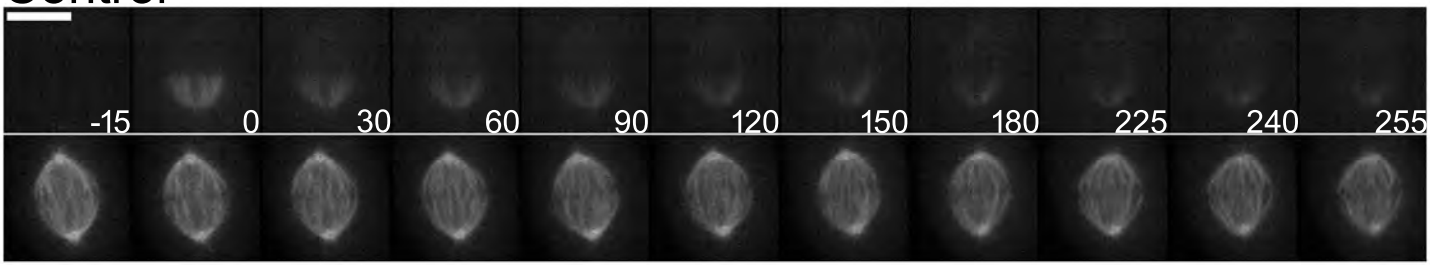

STLC

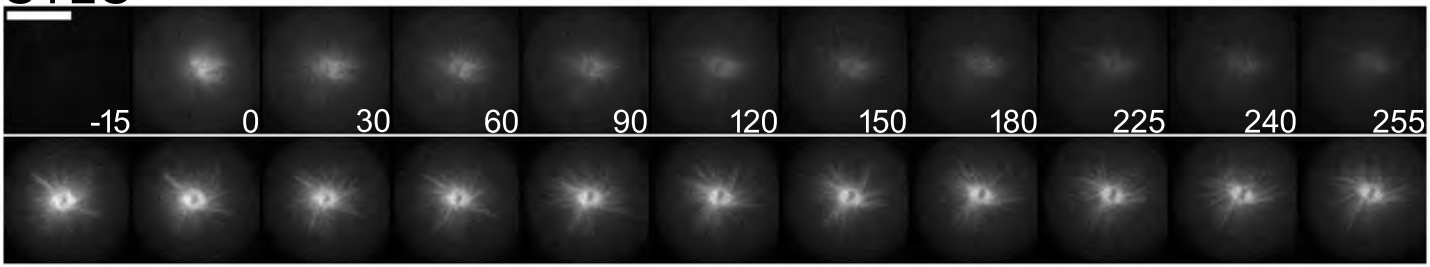

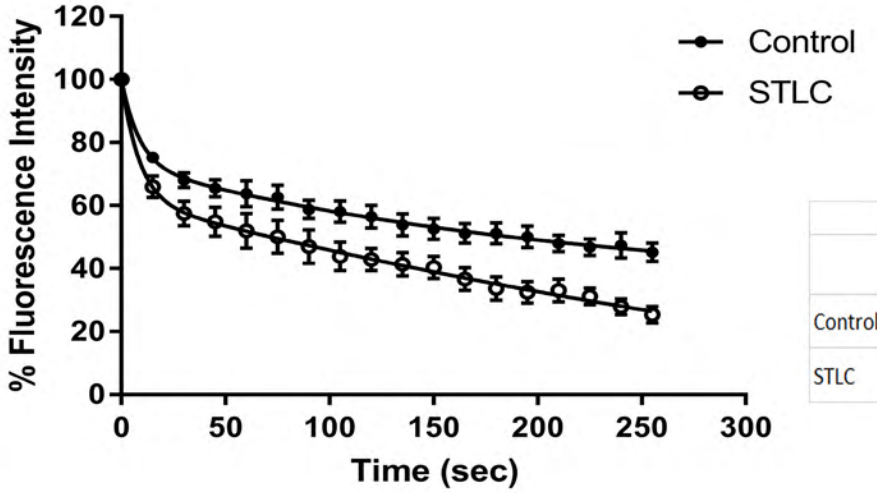

	Fast MT Population		Slow MT Population			
	%	$T_{1/2}$ (sec)	%	$T_{1/2}$ (min)	R^2	N
Control	30	7.3	70	6.4	0.997	19
STLC	37	5.3	64	3.5	0.997	20

Figure 2. Interpolar microtubules also comprise a portion of the slow turnover microtubule population. (Top) Select frames from live cell imaging of Tubulin photoactivation in U2OS cells stably expressing photoactivatable GFP-Tubulin and mCherry-Tubulin following treatment with either DMSO or 10 μm STLC to induce monopolar spindles. mCherry-Tubulin frames are from the mid-volume plane. Control cells were imaged at metaphase. Time, sec. Bar, 10 μm. (Bottom) Fluorescence dissipation after photoactivation. The filled and unfilled circles represent the average values recorded at each time point after photoactivation. Bars represent SEM. Control n = 19 cells, STLC n = 20 cells from four independent experiments. Lines indicate fitted curves (Control R^2 = 0.997; STLC R^2 = 0.997).

Figure 3

Control

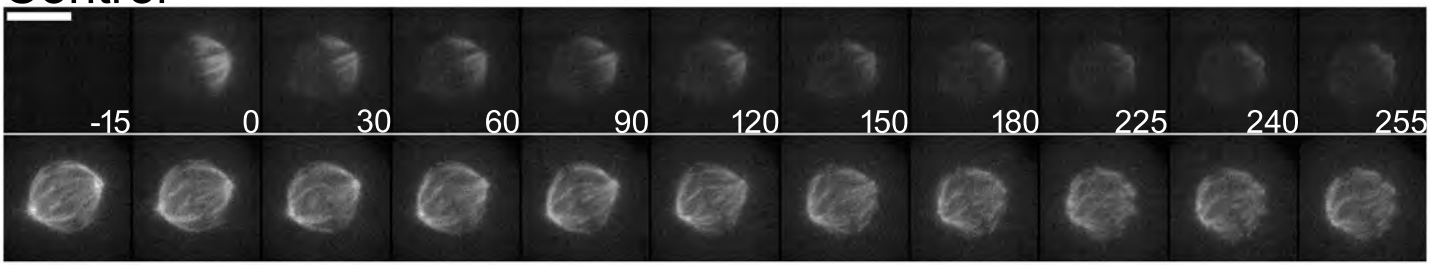

Low Temperature

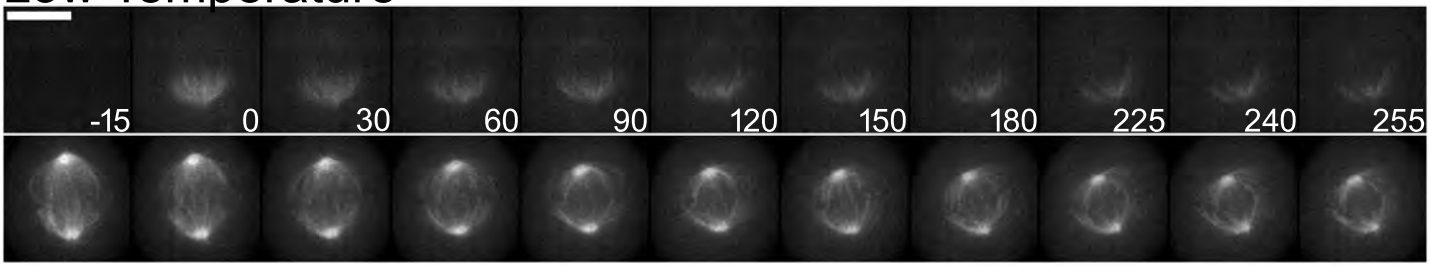

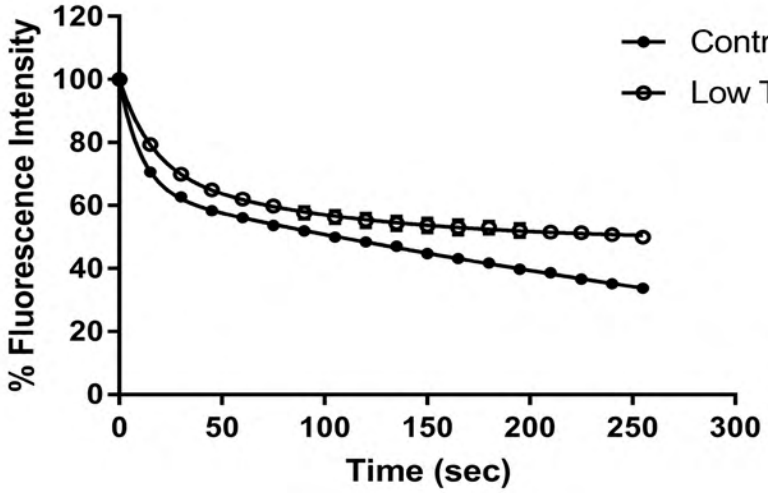

	Fast MT Population		Slow MT Population			
	%	$T_{1/2}$ (sec)	%	$T_{1/2}$ (min)	R^2	N
Control	35	7	65	4.6	0.999	21
Low Temp	38	15.7	61	14.4	0.998	27

Figure 3. Both fast turnover and slow turnover microtubule populations are sensitive to decreases in temperature. (Top) Select frames from live cell imaging of Tubulin photoactivation in U2OS cells stably expressing photoactivatable GFP-Tubulin and mCherry-Tubulin following imaging at 37°C (standard conditions) or at low temperature (22°C-25°C). mCherry-Tubulin frames are from the mid-volume plane. Cells were imaged at metaphase. Time, sec. Bar, 10 μm. (Bottom) Fluorescence dissipation after photoactivation. The filled and unfilled circles represent the average values recorded at each time point after photoactivation. Bars represent SEM. Control n = 21 cells, Low Temperature n = 27 cells from four independent experiments. Lines indicate fitted curves (Control R^2 = 0.999; Low Temperature R^2 = 0.998).

Figure 4

Control + MG132

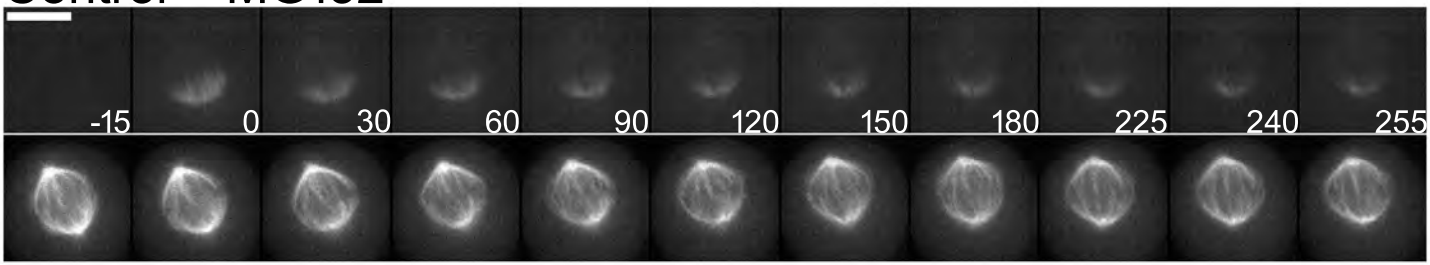

ZM447439 + MG132

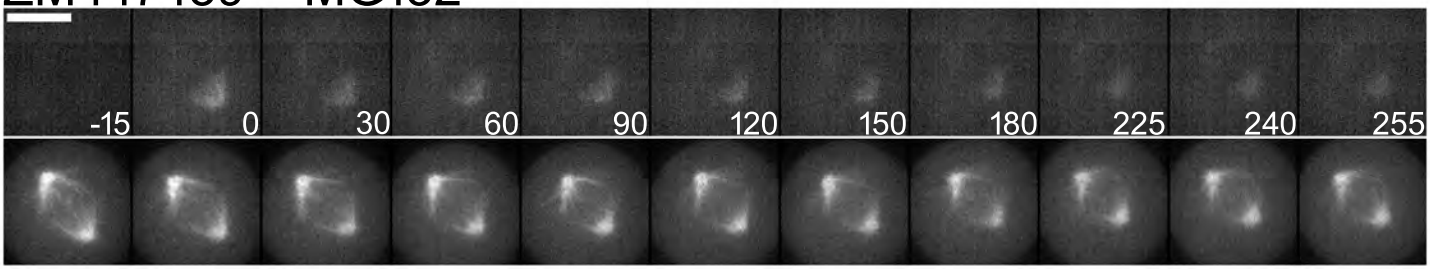

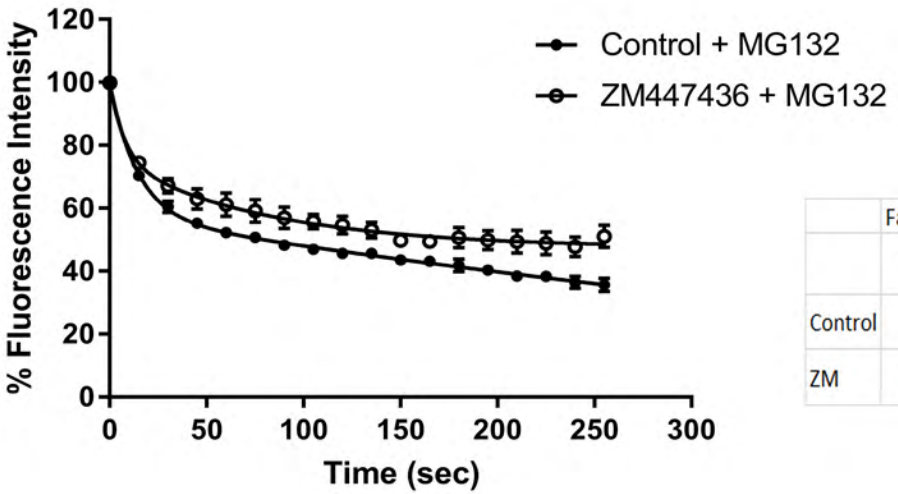

	Fast MT Population		Slow MT Population			
	%	$T_{1/2}$ (sec)	%	$T_{1/2}$ (min)	R^2	N
Control	42	9.8	58	6.1	0.999	20
ZM	37	11.1	63	10.5	0.984	19

Figure 4. Aurora B kinase inhibition affects slow microtubule population turnover. (Top) Select frames from live cell imaging of Tubulin photoactivation in U2OS cells stably expressing photoactivatable GFP-Tubulin and mCherry-Tubulin following treatment with either control DMSO or 3 μm ZM447439 to inhibit Aurora B activity along with 10 μm MG132. Control cells were imaged at metaphase. Time, sec. Bar, 10 μm. (Bottom) Fluorescence dissipation after photoactivation. The filled and unfilled circles represent the average values recorded at each time point after photoactivation. Bars represent SEM. Control n = 20 cells, ZM447439 n = 19 cells from three independent experiments. Lines indicate fitted curves (Control R^2 = 0.999; ZM447439 R^2 = 0.984).

Figure 5

Control RNAi + MG132

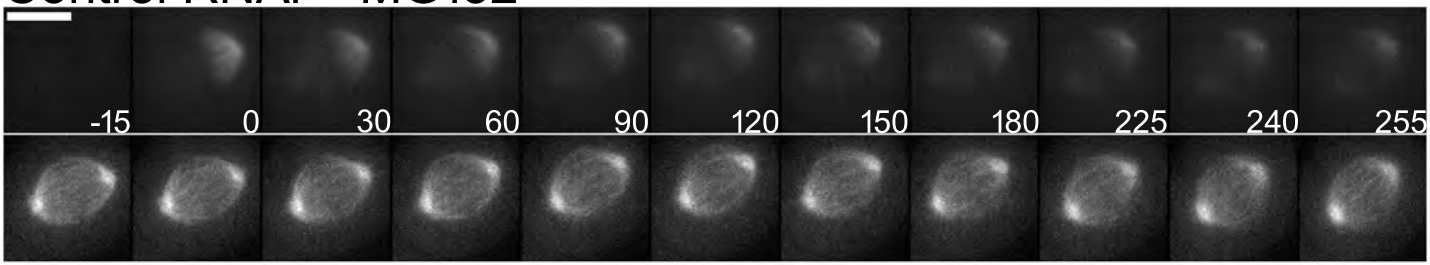

Hec1 RNAi + MG132 + ZM447439

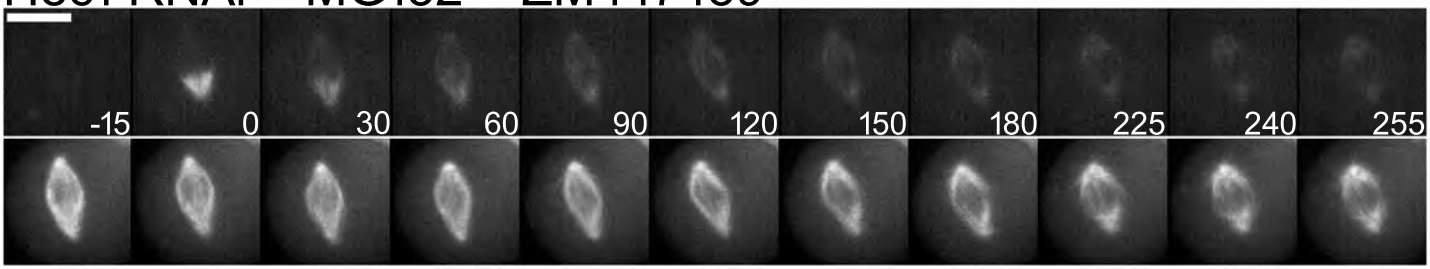

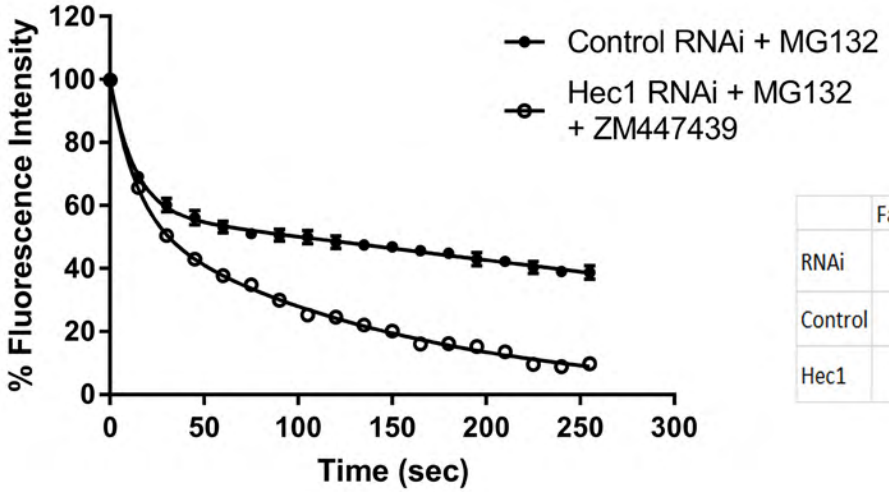

	Fast MT Population		Slow MT Population			
RNAi	%	$T_{1/2}$ (sec)	%	$T_{1/2}$ (min)	R^2	N
Control	41	8.5	59	7.2	0.998	19
Hec1	42	9.1	58	1.6	0.998	20

Figure 5. Aurora B kinase activity plays a role in enhancing spindle microtubule stability. (Top) Select frames from live cell imaging of Tubulin photoactivation in U2OS cells stably expressing photoactivatable GFP-Tubulin and mCherry-Tubulin following transfection with either control or Hec1 siRNA along with 10 μm MG132 treatment followed by DMSO or 3 μm ZM447439 to inhibit Aurora B activity. mCherry-Tubulin frames are from the mid-volume plane. Control cells were imaged at metaphase. Time, sec. Bar, 10 μm. (Bottom) Fluorescence dissipation after photoactivation. The filled and unfilled circles represent the average values recorded at each time point after photoactivation. Bars represent SEM. Control n = 19 cells, Hec1 + ZM447439 n = 20 cells from three independent experiments. Lines indicate fitted curves (Control RNAi R^2 = 0.999; Hec1 RNAi + ZM447439 R^2 = 0.998).

Figure S1

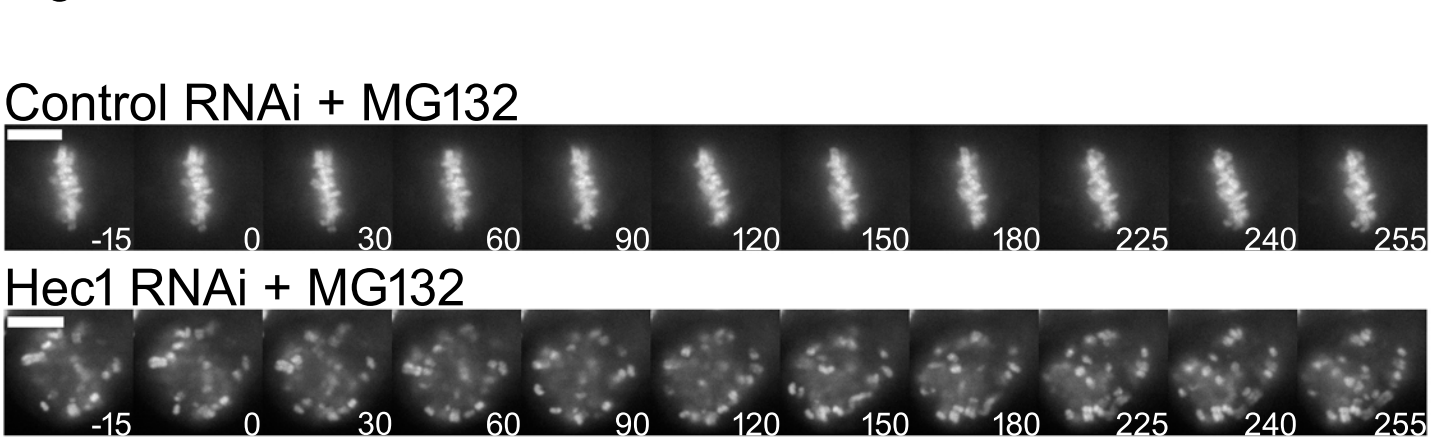
Control RNAi + MG132
-15
0
30
60
90
120
150
180
225
240
255
Hec1 RNAi + MG132
-15
0
30
60
90
120
150
180
225
240
255

Figure S1. Hec1 depletion phenotype. Select mid-volume frames of DNA labeled with SiR-DNA from cells treated as in Fig. 1 demonstrating Hec1 depletion phenotype with scattered chromosomes. Time, sec. Bar, 10 μm.

Figure S2

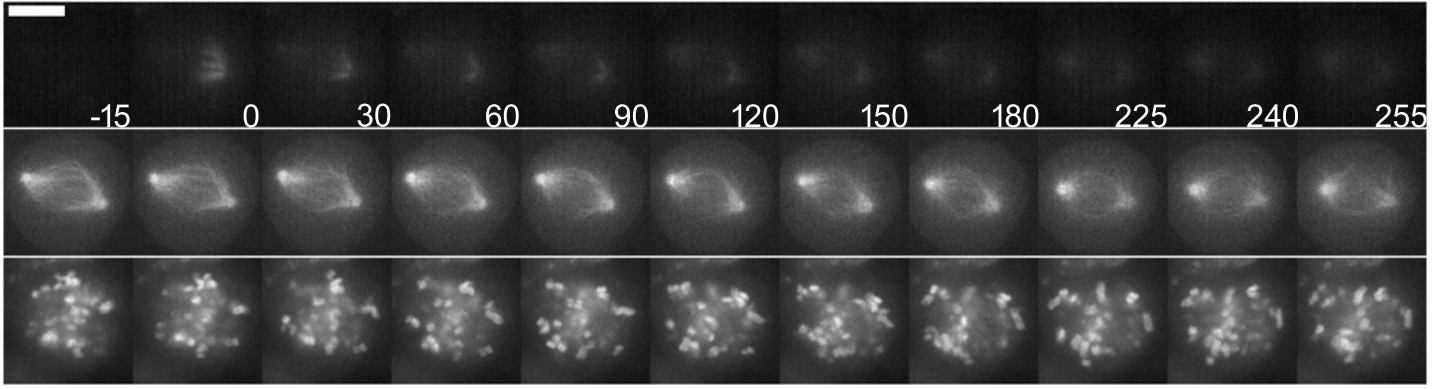

Figure S2. Spindle poles do not collapse in cells depleted of Hec1 following Eg5 inhibition. Select mid-volume frames from live cell imaging of Tubulin photoactivation in U2OS cells stably expressing photoactivatable GFP-Tubulin and mCherry-Tubulin following transfection with Hec1 siRNA along with 100 μm Monastrol and 10 μm MG132 treatment to prevent mitotic exit. Time, sec. Bar, 10 μm.